



## Article

# Synthesis and Characterization of Silver Nanoparticles for the Preparation of Chitosan Pellets and Their Application in Industrial Wastewater Disinfection

Paula Sartori <sup>1,2,3</sup>, Ana Paula Longaray Delamare <sup>2</sup>, Giovanna Machado <sup>4</sup> , Declan M. Devine <sup>3</sup>, Janaina S. Crespo <sup>1,3</sup> and Marcelo Giovanela <sup>1,\*</sup> 

<sup>1</sup> Área do Conhecimento de Ciências Exatas e Engenharias, Universidade de Caxias do Sul, Rua Francisco Getúlio Vargas, 1130, Caxias do Sul 95070-560, RS, Brazil

<sup>2</sup> Área do Conhecimento de Ciências da Vida, Instituto de Biotecnologia, Universidade de Caxias do Sul, Rua Francisco Getúlio Vargas, 1130, Caxias do Sul 95070-560, RS, Brazil

<sup>3</sup> PRISM Research Institute, Technological University of the Shannon (TUS), N37HD68 Athlone, Ireland

<sup>4</sup> Centro de Tecnologias Estratégicas do Nordeste, Ministério da Ciência, Tecnologia, Inovações e Comunicações, Av. Prof. Luis Freire, 01, Recife 50740-545, PE, Brazil

\* Correspondence: mgiovan1@ucs.br; Tel.: +55-54-3218-2159

**Abstract:** The use of silver nanoparticles (AgNPs) has become popular in several applications due to their bactericidal properties. In this sense, it is ideal that the AgNPs are incorporated into a matrix in order to minimize their release to the environment and to maintain their high reactivity. In view of these facts, the main goal of this work was to synthesize and characterize AgNPs, evaluating the influence of pH on the synthesis, for later incorporation into a chitosan polymeric matrix that will be used in the form of pellets for the disinfection of industrial wastewater. For this purpose, AgNPs were initially synthesized by a chemical route using silver nitrate, sodium borohydride and sodium citrate and then characterized by ultraviolet-visible spectroscopy, transmission electron microscopy and as a function of bacterial growth inhibition against *Escherichia coli* and *Enterococcus faecalis*. At the end of this procedure, AgNPs were incorporated in chitosan and the pellets formed were employed in the disinfection process, while assessing their bactericidal activity as well as the amount of silver leached. In general, the results showed that AgNPs synthesized at pH 10.0 were smaller ( $3.14 \pm 0.54$  nm) and presented greater dispersion than the AgNPs synthesized at other pH values. Furthermore, it was possible to observe a synergistic effect between chitosan and AgNPs and the chitosan pellets containing AgNPs proved to be effective in wastewater treatment, destroying *Escherichia coli* after 60 min of treatment. Finally, by considering the ease of application, the low environmental impact and the bactericidal action, it is concluded that the hybrid pellets developed in this work have great potential to be used as auxiliaries in wastewater treatment.

**Keywords:** silver nanoparticles; chitosan; wastewater treatment



**Citation:** Sartori, P.; Delamare, A.P.L.; Machado, G.; Devine, D.M.; Crespo, J.S.; Giovanela, M. Synthesis and Characterization of Silver Nanoparticles for the Preparation of Chitosan Pellets and Their Application in Industrial Wastewater Disinfection. *Water* **2023**, *15*, 190. <https://doi.org/10.3390/w15010190>

Academic Editors:  
Konstantinos Simeonidis and  
Kiriaki Kalaitzidou

Received: 30 November 2022

Revised: 24 December 2022

Accepted: 29 December 2022

Published: 2 January 2023



**Copyright:** © 2023 by the authors. Licensee MDPI, Basel, Switzerland. This article is an open access article distributed under the terms and conditions of the Creative Commons Attribution (CC BY) license (<https://creativecommons.org/licenses/by/4.0/>).

## 1. Introduction

Metallic nanoparticles are materials whose size varies between 1 and 100 nm, and which have different properties in relation to the source metal [1]. They have unique properties due to their size, shape, composition, higher surface area to volume ratio, and purity of constituents. These properties allow these materials to be used in drug delivery systems, wastewater disinfection, catalysts and as remediation agents for various pollutants [2]. In this context, different nanoparticles have been studied, e.g., copper nanoparticles (CuNPs), zinc oxide nanoparticles (ZnONPs), titanium dioxide nanoparticles (TiO<sub>2</sub>NPs), gold nanoparticles (AuNPs), silver nanoparticles (AgNPs) and others [2–5].

AgNPs can be obtained through chemical, physical and biological methods [6,7], and come in different sizes and shapes (cubic, triangular, spherical, prismatic, wire or bars, etc.)

These characteristics are directly influenced by the synthesis method used [8]. In addition, parameters such as temperature, time, pH, concentration of the reducing agent and concentration of the precursor metal salt also influence the shape, size and texture of AgNPs [2,9]. These nanoparticles have very interesting biological properties, from broad-spectrum antibacterial action to antiviral and anticancer activities [10–13]. As they inhibit bacterial growth and have high bactericidal activity [14], the use of AgNPs has become popular in several applications, such as health, the textile industry, food packaging and wastewater treatment [15–19]. Wastewater treatment is very important, as the need for pure water is increasing and the incorrect disposal of effluents is an environmental challenge [20,21]. Nanotechnology has arisen as a new technology extremely important for the treatment of wastewater. Nanoparticles can be used as absorbents for the removal of heavy metals [22] and other processes, such as catalytic oxidation, membrane filtration and disinfection, and different kinds of nanoparticles can be used depending on the goal of the treatment [23]. Studies carried out using AgNPs for wastewater treatment have shown that this technology is effective for the inhibition of the bacteria present in wastewater [24–26].

The toxicity of AgNPs can limit their application, so it is important to control their release to the environment [18,27]. Ideally, nanomaterials should be incorporated into a matrix, in order to minimize their release to the environment and maintain high reactivity, since they can become pollutants if not collected after use. In this way, material matrices that are renewable, sustainable and biodegradable should be used [28]. Thus, the use of polymeric matrices combined with AgNPs is quite promising due to their porosity, which promotes better access to reagents and a greater surface area [29].

The use of natural polymers, such as chitosan, for the manufacture of hybrid systems containing metallic nanoparticles in environmental remediation processes has advantages over synthetic polymers, as they are abundant, have low economic value and are environmentally friendly [30]. Chitosan is an excellent option for the preparation of hybrid systems with AgNPs, presenting a high disinfection capacity [31]. Research carried out with these hybrid systems generally involves the production of pellets, films, sponges and microspheres for use in different applications, such as wastewater treatment, food packaging and medical products [27,32–40]. The improvements in the mechanical properties of chitosan when forming a hybrid system with AgNPs and the synergistic effect of these materials on bactericidal activity, indicate that research in the area should be further explored, evaluating different parameters to optimize the processes and obtain increasingly satisfactory results. Therefore, the objective of this work was to prepare chitosan-based hybrid systems containing AgNPs for later use in wastewater disinfection, with a short coculturing period and promoting not only the inhibition, but also the elimination of *Escherichia coli*.

## 2. Materials and Methods

### 2.1. Materials and Chemicals

Silver nitrate was synthesized from silver recovered from button cell batteries, as described in a previous work [41]. For the synthesis of AgNPs, sodium borohydride, hydrochloric acid, sodium hydroxide (Merck, Saint Louis, MO, USA) and sodium citrate (Sigma-Aldrich, Saint Louis, MO, USA) were used. Chitosan pellets were produced with high molecular weight chitosan (Sigma-Aldrich), 100% glacial acetic acid (Merck) and 50% *w/v* glutaraldehyde (Sigma Aldrich). All materials were used as received.

All solutions were prepared with deionized water ( $\rho > 18.2 \text{ M}\Omega \text{ cm}$ ; Direct-Q 3 UV, Millipore, Darmstadt, Germany).

The wastewater sample was collected in the treatment plant for the stainless-steel cutlery industry in the municipality of Farroupilha (in the northeast region of Rio Grande do Sul state, Brazil). The raw wastewater was characterized in a previous work [24]. This wastewater consisted of the water used to clean parts, in the gas scrubber and in the kitchen, and it underwent a physical–chemical treatment to remove solids, before being mixed with a sanitary effluent in a biological treatment tank to remove organic matter.

The water resulting from this last stage was then taken to a reservoir, where it was mixed with rainwater.

## 2.2. Methods

AgNPs were synthesized at different pH values and the solutions were evaluated by UV-Vis, TEM and by its antimicrobial properties. Then, the optimal AgNPs solution was added to chitosan to produce pellets. The pellets were also evaluated by their antimicrobial properties. The pellets of chitosan containing AgNPs were compared with pellets of pure chitosan, since chitosan itself also presents antibacterial properties. The pellets of chitosan-containing AgNPs were used in the disinfection of industrial wastewater that was later evaluated by the presence of *Escherichia coli* by Petrifilm 3M<sup>®</sup> assay. In order to verify if the treatment with the pellets of chitosan-containing AgNPs was bacteriostatic or bactericidal against *Escherichia coli*, the same treatment was performed in a solution with only this bacterium. Figure 1 presents a schematic diagram of the methodology of this study.

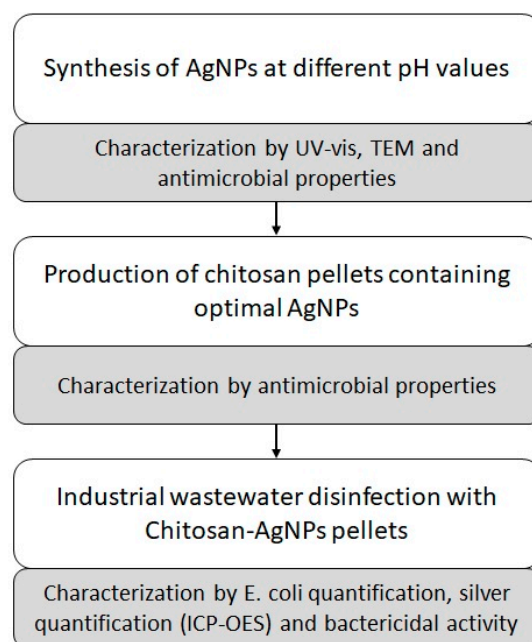


**Figure 1.** Schematic diagram of the methodology of the study.

## 2.3. AgNPs Synthesis

The synthesis of AgNPs was based on the method proposed by Jana et al. (2001) [42]. Briefly, a solution of  $\text{AgNO}_3$   $2.5 \text{ mmol L}^{-1}$ , a solution of sodium borohydride  $5.0 \text{ mmol L}^{-1}$  and a solution of sodium citrate  $2.5 \text{ mmol L}^{-1}$  were used. The pH of the sodium citrate solution was varied from 2.0 to 13.0, with previously prepared solutions of  $\text{HCl}$   $0.1 \text{ mol L}^{-1}$  or  $\text{NaOH}$   $0.1 \text{ mol L}^{-1}$ . The concentration of the sodium citrate solution was kept the same as that of  $\text{AgNO}_3$ , based on the work of Henglein and Giersig (1999) [43].

For the synthesis of AgNPs, 10.0 mL of  $\text{AgNO}_3$  solution were added to 10.0 mL of each sodium citrate solution, at room temperature and protected from light, under manual stirring. Then, 0.6 mL of the sodium borohydride solution was added and stirred for 1 min.

## 2.4. Characterization of AgNPs

### 2.4.1. UV-Vis Spectroscopy

The AgNPs were characterized by molecular absorption spectroscopy in the UV-Vis region (in Beckman DU 530 equipment), from 300 to 600 nm and with steps of 1.0 nm, using a quartz cuvette with a 1.0 cm optical path.

#### 2.4.2. Transmission Electronic Microscopy (TEM)

Samples of AgNPs solutions were diluted in deionized water and one drop was deposited on a holey carbon grid. Samples were analyzed by TEM (MORGAGNI 268 D, FEI Company, Hillsboro, USA), with an acceleration voltage of 80 kV. The size of AgNPs was analyzed with ImageJ software (version 1.53).

#### 2.4.3. Inhibition of Bacterial Growth

AgNPs were also evaluated in terms of their ability to inhibit bacterial growth. *Escherichia coli* (Gram-negative) and *Enterococcus faecalis* (Gram-positive), at a concentration of  $1.0 \times 10^8$  CFU mL<sup>-1</sup>, were inoculated into Petri dishes with agar. To these, three drops (5.0 µL) of each AgNPs solution were placed on the plates and these were incubated for 24 h at 37 °C in an incubator. At the end of the incubation period, the formation of inhibition halos was observed in the places where the AgNPs solutions were placed, and the colony formed unit (CFU) within these inhibition halos was counted with the aid of a magnifying glass.

#### 2.5. Preparation and Evaluation of Chitosan and AgNPs Pellets

Optimal AgNPs, which showed the greatest potential for the inhibition of bacterial growth, were used to produce chitosan pellets. A solution of 1.5% *w/v* of chitosan was prepared by suspending chitosan in 0.20 mol L<sup>-1</sup> acetic acid. After 24 h, 3.0 mL of AgNPs solution and 60.0 µL of 50% (*w/v*) glutaraldehyde were added to 7.0 g of chitosan solution. The solution was homogenized and dripped into a Petri dish with a syringe containing a 1.5 mol L<sup>-1</sup> NaOH solution to form the pellets.

Chitosan pellets containing AgNPs were then deposited on Petri dishes, with the same bacteria and conditions described above. After the incubation period, the diameter of the inhibition halo formed around the pellets was evaluated. For comparison purposes, the procedure was also performed with pellets produced only with chitosan, using deionized water instead of the AgNPs solution to maintain the same proportions.

#### 2.6. Wastewater Disinfection

The industrial wastewater disinfection process consisted of stirring 150.0 mL of wastewater with 50 pellets of chitosan-containing AgNPs, for periods of 60, 120 and 180 min at room temperature. The assay was performed in duplicate using a shaker incubator (715D, Novatecnica, Piracicaba, Brazil), with a stirring frequency of 150 rpm. Before the assay and at the end of each period, an aliquot of about 1.0 mL of the wastewater was collected to perform the quantification of *Escherichia coli* by Petrifilm 3M<sup>®</sup>, using method 991.14, adopted by the Association of Official Analytical Chemists (AOAC, 2016) [44].

#### Inductively Coupled Plasma Optical Emission Spectroscopy (ICP-OES)

The quantification of silver leached in the wastewater disinfection process was performed with raw effluent and with an aliquot of the treated wastewater, after a period of 180 min, by inductively coupled plasma optical emission spectroscopy (ICP-OES), using the Standard Methods 3120B for Examination of Water and Wastewater (2017) [45].

#### 2.7. Bactericidal Activity of Chitosan and AgNPs Pellets

In order to verify whether the disinfection process had a bacteriostatic or bactericidal action against *Escherichia coli*, 150.0 mL of a solution containing this bacterium, at a concentration of  $7.9 \times 10^2$  (which was equal to the average concentration of the wastewater), was treated with the same parameters used in the wastewater disinfection.

Aliquots of the solution were collected after 60, 120 and 180 min of treatment and inoculated into Petri dishes. Subsequently, the plates were incubated in a bacteriological oven at 37 °C for 24 h, prior to the assessment of bacterial growth on the incubated plates.

### 3. Results and Discussion

#### 3.1. Synthesis and Characterization of AgNPs

The visual appearances of the AgNPs obtained from the  $\text{AgNO}_3$  solution, with a concentration of  $2.5 \text{ mmol L}^{-1}$  and pH variation of the sodium citrate solution from 2.0–13.0, are shown in Figure 2.

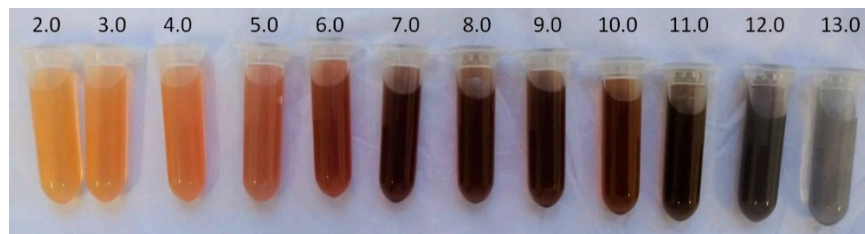


**Figure 2.** Visual aspect of AgNPs synthesized as a function of the pH of the sodium citrate solution.

As can be observed in Figure 2, the color intensity of the solutions increased from yellow to brown with increasing pH, except for pH 13.0, in which a dark grey solid precipitate was observed. This phenomenon can be explained based on the Pourbaix diagram for silver [46], in which it is verified that aqueous solutions with  $\text{pH} > 12.0$  witness the formation of silver hydroxide ( $\text{AgOH}$ ) and the precipitation of silver oxides. Norouzi et al. (2020) [47] designed a Pourbaix diagram for the  $\text{Ag-HNO}_3\text{-H}_2\text{O}$  system with MEDUSA software, where it was also possible to verify that silver oxides precipitate at high pH values.

The UV-Vis spectra of the AgNPs solutions are shown in Figure 3. Absorbance values greater than 1.0 were due to the fact that the spectra were obtained using the same correction factor with which the solutions were diluted. In this way, it was possible to compare all spectra in the same figure. Figure 4 presents the TEM images of the solutions of AgNPs and the histograms are shown in Figure 5.

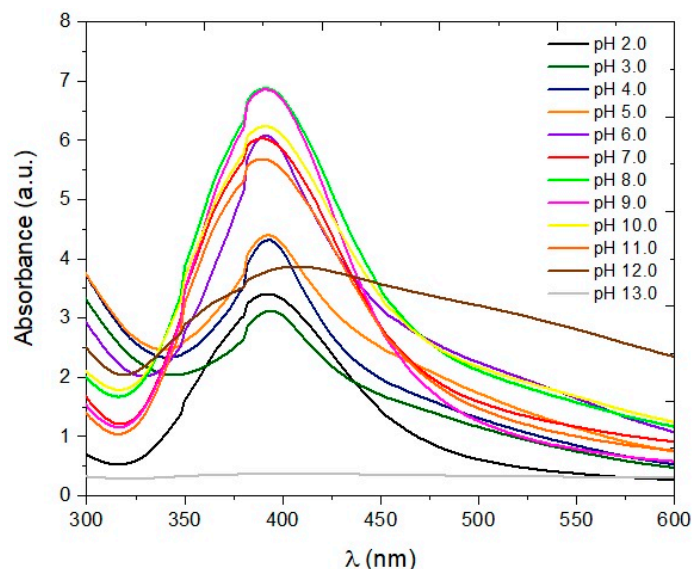


**Figure 3.** UV-Vis spectra of AgNPs synthesized at different pH values of sodium citrate solution.

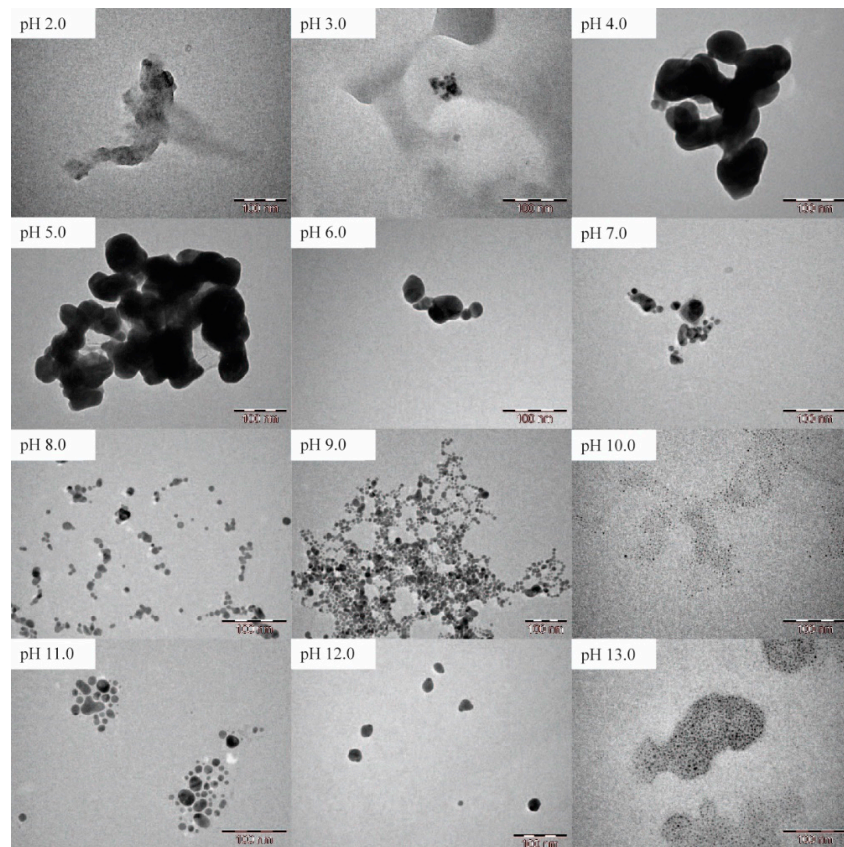


**Figure 4.** TEM images obtained from dilute solutions of AgNPs synthesized at the pH range 2.0–13.0. All images are scaled to 100 nm.

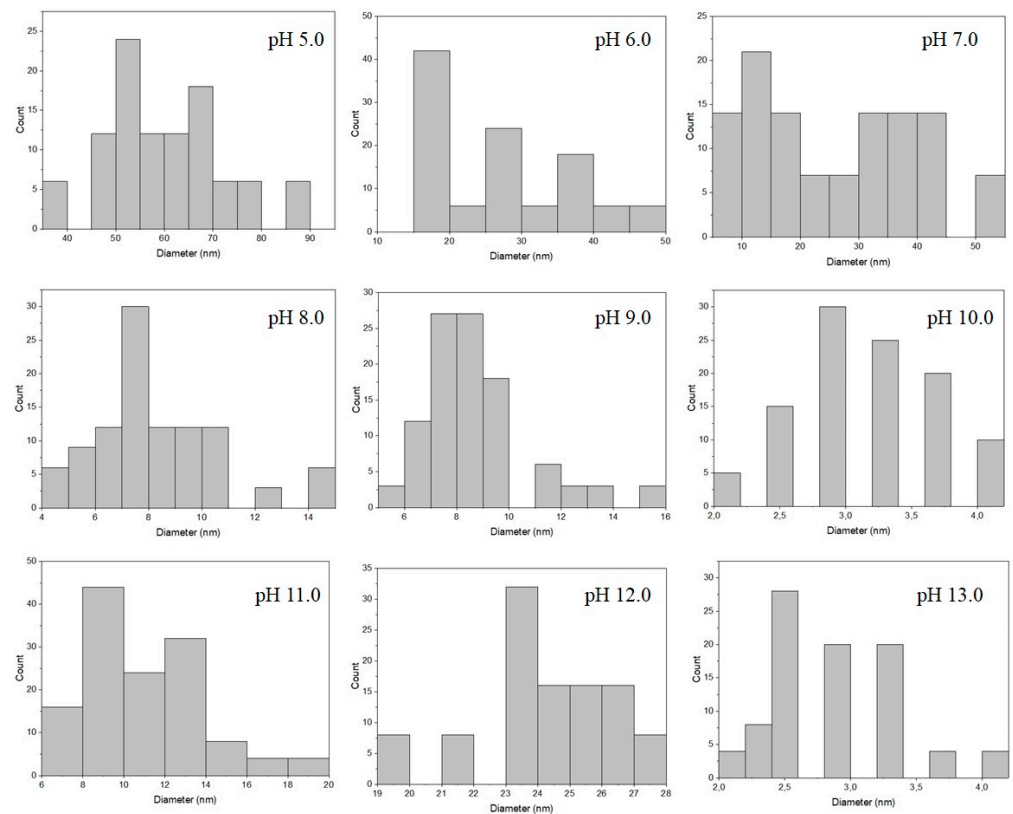


**Figure 5.** Histograms of AgNPs synthesized at pH range 5.0–13.0.

The solution of pH 13.0 did not show a maximum absorption ( $\lambda_{\max}$ ) around 400 nm, indicating that there were no AgNPs. Despite this, the TEM image shows the presence of some clustered AgNPs. As this solution showed the precipitation of a dark grey solid at the time of synthesis, it was not diluted for further testing and, thus, the actual amount of AgNPs was lower than that observed in the other solutions, which were diluted.

The spectra of the more acidic solutions, with  $\text{pH} < 5.0$ , showed lower intensity. Biao et al. (2017) [48] observed that the pH of the medium directly influences the size and shape of AgNPs, and AgNPs synthesized at pH 4.0 are relatively larger than those synthesized at pH 5.0. Furthermore, AgNPs synthesized at pH 4.0 present a triangular shape, while those synthesized at pH 5.0 are spherical. In the TEM images, it can be seen that the AgNPs synthesized at pH 2.0 and 3.0 did not have a specific shape, while the AgNPs synthesized at pH 4.0 and 5.0 had well-defined contours but were agglomerated. For these reasons, it was not possible to obtain a histogram of the AgNPs synthesized at pHs 2.0, 3.0 and 4.0. Fu et al. (2021) [9] observed that the absorbance of AgNPs decreased in acidic solutions and increased in alkaline solutions, since AgNPs are more stable in an alkaline environment. Zhao et al. (2022) [49] observed that a high pH tends to result in a high reduction rate of silver ions and a high formation rate of AgNPs.

The UV-Vis spectra of solutions with pH between 6.0 and 11.0 showed similar behavior, exhibiting a relatively intense absorbance, with  $\lambda_{\max}$  around 390 nm, which may indicate spherical [50] or small [51] AgNPs. Comparing the UV-Vis spectra of AgNPs (Figure 3) with those simulated by Bertin and Perottoni (2020) [52], using the Mie model for spherical particles, it can be assumed that the synthesized AgNPs had a particle size between 5 and 20 nm. The width of the bands also indicated that the particle size distribution was similar for all samples tested [53]. TEM images confirmed the spherical shape of these AgNPs, but it was observed that the pH still influenced the size and dispersion of AgNPs. According to Dong et al. (2009) [54], the pH of the solution can affect the size and shape of AgNPs, since the reducing activity of sodium citrate is pH-dependent. From pH 7.0, the citrate structure is fully ionized [55] and has a stronger solvation capacity [56], which may explain the better dispersion of AgNPs in higher pH ranges. Salazar-Bryam et al. (2021) [57] also observed that at higher pH values, the size and shape of AgNPs were more uniform. The histograms demonstrate that, as the pH increased, the size of the AgNPs decreased, but to pH 11.0 and pH 12.0, it is possible to observe that the size of AgNPs increased again and they lost stability and precipitate at pH 13.0.

AgNPs synthesized at pH 10.0 exhibited the smallest size ( $3.14 \pm 0.54$  nm) and the greatest dispersion. Mohaghegh et al. (2020) [58] synthesized AgNPs, evaluating the type of reducing agent and its concentrations, pH and temperature of the medium. In their work, it was possible to observe that the UV-Vis spectra of AgNPs solutions synthesized at pH 10.0 remained stable, regardless of other factors, such as temperature, reducing agent and concentration, while the UV-Vis spectra of AgNPs synthesized in other pH values underwent significant changes in relation to the shape and intensity of the absorption bands. The authors concluded that at pH 10.0, it is possible to synthesize spherical and stable AgNPs with a more uniform particle size distribution. Raota et al. (2019) [32] observed that AgNPs synthesized from grape pomace extract with pH 10.0 were spherical, dispersed and had a smaller average particle diameter, which implies a greater surface area and, consequently, greater bactericidal activity.

After evaluating the UV-Vis spectra and TEM images of AgNPs synthesized with  $\text{AgNO}_3$  at a concentration of  $2.5 \text{ mmol L}^{-1}$ , it was decided to also synthesize AgNPs with  $\text{AgNO}_3$  concentrations of  $1.25$  and  $5.0 \text{ mmol L}^{-1}$ , at pH 10.0, to compare the three solutions in terms of bacterial growth inhibition. The solutions were dripped onto Petri dishes, where *Escherichia coli* and *Enterococcus faecalis* bacteria were inoculated.

Table 1 presents the result of the CFU counts from Petri dishes of *Escherichia coli*. No changes were observed in the diameter of the formed halos, which corresponded to the size of the droplets. Based on the data presented, it was observed that AgNPs obtained with the solution of  $\text{AgNO}_3$  in the concentration of  $5.0 \text{ mmol L}^{-1}$  presented the best results of the inhibition of bacterial growth.

**Table 1.** CFU count in inhibition halos formed by AgNPs synthesized at pH 10.0 in Petri dishes inoculated with *Escherichia coli*.

[ $\text{AgNO}_3$ ] ( $\text{mmol L}^{-1}$ )	Assay 1	Assay 2	Assay 3
1.25	>20	>20	>20
2.50	10	>20	>20
5.00	5	5	5

In the Petri dishes in which *Enterococcus faecalis* was inoculated, the formation of inhibition halos was not observed in the places where the AgNPs solutions were dripped. AgNPs were not as effective at inhibiting the growth of Gram-positive bacteria when compared to inhibiting the growth of Gram-negative bacteria. This is due to the structural difference in the cell wall of each type of bacteria [59]. Gram-positive bacteria have a peptidoglycan layer, which is the key component of the cell wall, located immediately outside the cytoplasmic membrane, and about 30 nm thick; Gram-negative bacteria have a peptidoglycan layer of 2–3 nm [31]. Thus, AgNPs are unable to cross the peptidoglycan layer of Gram-positive bacteria and attack the interior of cells.

### 3.2. Evaluation of Chitosan and AgNPs Pellets

AgNPs solution synthesized at pH 10.0, from an  $\text{AgNO}_3$  solution with a concentration of  $5.0 \text{ mmol L}^{-1}$ , was used to produce the chitosan pellets, since they have the greatest ability to inhibit bacterial growth. The average diameter of the inhibition halos formed by chitosan and chitosan pellets with AgNPs is shown in Table 2.

**Table 2.** Mean diameter of inhibition halos (mm) formed by chitosan pellets and chitosan pellets containing AgNPs.

	<i>Escherichia coli</i>	<i>Enterococcus faecalis</i>
Chitosan	$7.72 \pm 0.10$	$6.98 \pm 0.37$
Chitosan + AgNPs	$8.10 \pm 0.62$	$6.23 \pm 0.84$

These results show that the mean diameter of the halos formed in the Petri dish with *Enterococcus faecalis* was smaller for the chitosan pellets containing AgNPs than for those of pure chitosan. This result, however, does not imply that the addition of AgNPs negatively interfered with the bactericidal action of chitosan. Some researchers have demonstrated that films produced with chitosan showed an increase in tensile strength when AgNPs were incorporated [27,33,34,37,38,40]. The main reason for the increase in tensile strength is due to the strong interaction between the polymer matrix and the nanoparticles caused by the formation of intermolecular bonds [34,60]. In a pellet, the increase in tensile strength can increase the contact angle with the surface, since chitosan and AgNPs form a more compact structure [33,38] and the pellet becomes more rigid. Thus, the contact angle between the chitosan pellet containing AgNPs and the sample was greater than the contact angle between the pure chitosan pellet and the sample, as shown in Figure 6.



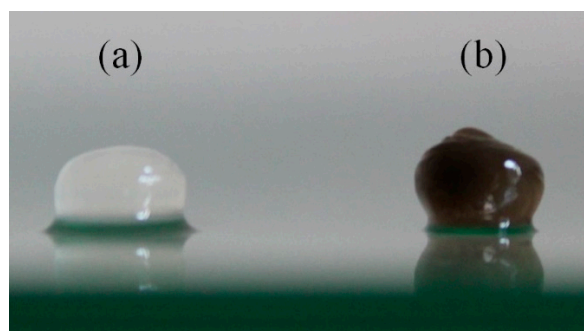


**Figure 6.** Contact angle with the surface of (a) chitosan and (b) chitosan with AgNPs pellets.

This image was evaluated with Adobe Illustrator software, and it was found that the contact area with the surface of the chitosan pellet containing AgNPs was 18% smaller in relation to the contact with the surface of the pure chitosan pellet. Thus, one explanation for the observed phenomenon is that the halo formed by the chitosan pellet containing AgNPs was smaller, as a smaller area of the pellet was in contact with the sample, compared to the pure chitosan pellet.

Taking into account the standard deviation of the measurements, the inhibition halo formed by the pure chitosan pellets and the chitosan pellets containing AgNPs was practically the same, despite the chitosan pellets with AgNPs being in contact with an area of the sample 18% smaller than pure chitosan pellets, which indicates a synergistic effect between chitosan and AgNPs [61]. This effect can be explained by the antimicrobial activity of each material. The positively charged chitosan interacts electrostatically with the negatively charged bacteria cell wall, which leads to a change in cell membrane permeability [62,63]. In turn, the main target of AgNPs is the cytoplasmic membrane [64], which can be reached more easily if the cell wall is compromised.

### 3.3. Industrial Wastewater Disinfection

Table 3 presents the values of *Escherichia coli* quantification of the wastewater before and after the treatment with the chitosan pellets containing AgNPs.

**Table 3.** Quantitative determination of *Escherichia coli* (CFU mL<sup>-1</sup>) in raw wastewater and wastewater treated with chitosan pellets containing AgNPs.

	Assay 1	Assay 2
Raw wastewater	$8.2 \times 10^2$	$7.6 \times 10^2$
60 min of treatment	<LQ *	<LQ
120 min of treatment	<LQ	<LQ
180 min of treatment	<LQ	<LQ

Note: \* LQ = limit of quantification (1.0 CFU).

After 60 min of treatment, it was no longer possible to detect *Escherichia coli* in the treated industrial wastewater, demonstrating the high antibacterial activity of chitosan pellets containing AgNPs. Some authors have reported positive results in the treatment of industrial wastewaters with hybrid materials. The use of AgNPs in the preparation of these hybrids is a common feature of these works. Raota et al. (2019) [32] observed a 47% reduction in *Escherichia coli* count in industrial wastewater, after 60 min of treatment with chitosan pellets containing AgNPs synthesized from grape pomace extract. In another work, Zarpelon et al. (2016) [65] treated industrial wastewater with thin films of poly(allylamine hydrochloride) (PAH) and poly(acrylic acid) (PAA) containing AgNPs and, after 360 min, observed a 90% reduction in the *Escherichia coli* count. The authors also performed a second treatment cycle, where the reduction was 93% due to the greater amount of silver leached into the medium. Lovatel et al. (2015) [66] used hybrids of montmorillonite, alginate and

AgNPs to treat industrial wastewater and observed a 98.5% reduction in total coliforms after 90 min of treatment.

Regarding the quantification of leached silver, Table 4 summarizes the concentrations observed for the wastewater before treatment and after 180 min. As can be seen, silver was only detected in one of the test repetitions.

**Table 4.** Quantitative determination of silver ( $\text{mg L}^{-1}$ ) in raw wastewater and wastewater treated with chitosan pellets containing AgNPs, by inductively coupled plasma optical emission spectroscopy (ICP-OES).

	Assay 1	Assay 2
Raw wastewater	<LQ *	<LQ
180 min of treatment	<LQ	0.0113

Note: \* LQ = limit of quantification ( $0.0093 \text{ mg mL}^{-1}$ ).

According to the drinking-water quality guidelines of the World Health Organization (WHO, 2022) [67], a reference value of concentration for silver in drinking-water, which does not pose a risk to human health, is  $0.1 \text{ mg L}^{-1}$ . The amount of silver leached in the assay was almost 10 times lower than the reference value; therefore, it did not indicate risks to human health.

#### 3.4. Bactericidal Activity of Chitosan and AgNPs Pellets

Figure 7 shows the results of the assay to evaluate the bactericidal activity of chitosan pellets containing AgNPs. There was no growth of *Escherichia coli* in the Petri dishes, where the solution was incubated after the disinfection process with chitosan pellets containing AgNPs.

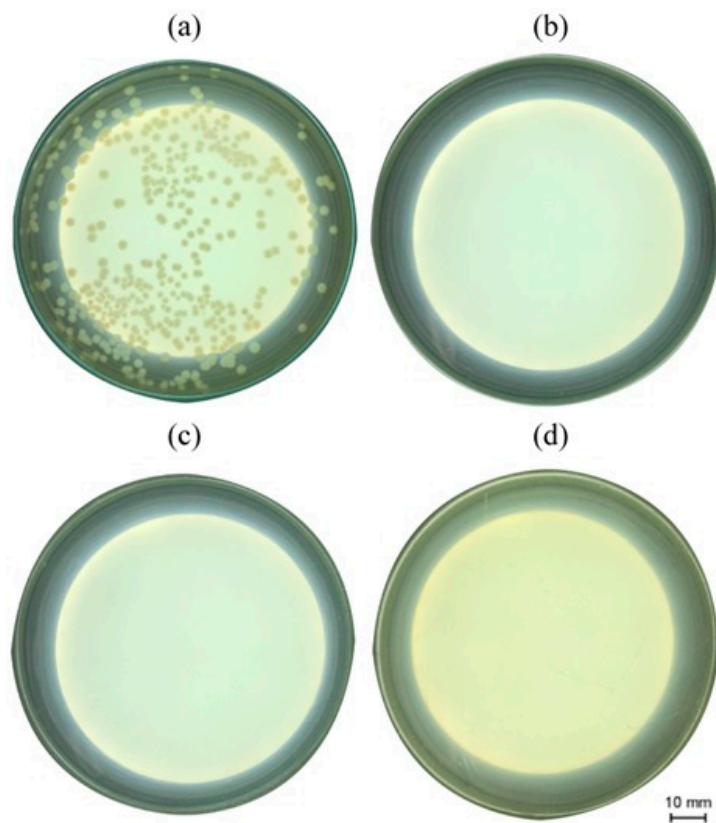


**Figure 7.** Evaluation of the bactericidal activity of chitosan pellets containing AgNPs against *Escherichia coli*: (a) control; (b) 60 min of treatment; (c) 120 min of treatment; (d) 180 min of treatment.

The results obtained at this stage clearly demonstrate that the treatment of wastewater with chitosan pellets containing AgNPs was effective and had a bactericidal effect against *Escherichia coli* after 60 min of incubation.

#### 4. Conclusions

In this work, AgNPs were synthesized, characterized and later incorporated in a chitosan polymeric matrix to form pellets with a view to utilizing them in the disinfection of industrial wastewater.

In general, the pH strongly influenced the synthesis of AgNPs. Those synthesized between pH 6.0 and pH 11.0 showed similar UV-Vis spectra, with greater intensity than the AgNPs synthesized at other pH values. The intensities of the spectra of the solutions at pH < 5.0 were much lower. However, a characteristic  $\lambda_{\max}$  was not observed for the solution of AgNPs synthesized at pH 13.0, in which a dark grey solid, possibly silver oxide, precipitated. AgNPs synthesized at pH 10.0 showed the smallest size ( $3.14 \pm 0.54$  nm), greatest dispersion and the ability to inhibit bacterial growth against *Escherichia coli*. It was shown that the higher the concentration of AgNPs, the greater the inhibition of bacterial growth.

Chitosan pellets containing AgNPs showed good bacterial growth inhibition results for both *Escherichia coli* and *Enterococcus faecalis*. The synergistic effect of chitosan and AgNPs was also observed, since the chitosan pellets containing AgNPs were more rigid and their contact with the surface was 18% smaller than the pellets of pure chitosan; the inhibition halo formed by both pellets was practically the same. The wastewater treatment with chitosan pellets containing AgNPs proved to be effective. *Escherichia coli* present in the wastewater was completely eliminated in just 60 min of treatment. A small amount of silver was leached into the treated wastewater but in a low concentration that did not indicate risks to human health or the environment.

Finally, it can be concluded that the synthesized AgNPs had bactericidal activity and could be incorporated into a chitosan polymeric matrix, to form a hybrid material to deactivate or destroy bacteria. The treatment of wastewater with chitosan pellets containing AgNPs is effective and has the capacity to destroy *Escherichia coli* after short coculturing periods. Since the hybrid material presented in this study has shown great bactericidal activity, it may be further studied and used in other fields, such as water filters, food storage and wound dressings.

**Author Contributions:** P.S.: Conceptualization, Methodology, Validation, Investigation, Writing—Original draft preparation, Writing—Reviewing and Editing, Visualization; A.P.L.D.: Investigation, Writing—Original draft preparation; G.M.: Investigation, Writing—Original draft preparation; D.M.D.: Writing—Original draft preparation, Writing—Reviewing and Editing; J.S.C.: Writing—Original draft preparation, Writing—Reviewing and Editing, Visualization, Supervision, Funding acquisition; M.G.: Writing—Original draft preparation, Writing—Reviewing and Editing, Visualization, Supervision, Funding acquisition. All authors have read and agreed to the published version of the manuscript.

**Funding:** This research received financial support from CAPES (Finance code—001).

**Data Availability Statement:** The data presented in this study are available within the article.

**Conflicts of Interest:** The authors declare no conflict of interest.

#### References

1. Jamkhande, P.G.; Ghule, N.W.; Bamer, A.H.; Kalaskar, M.G. Metal Nanoparticles Synthesis: An Overview on Methods of Preparation, Advantages and Disadvantages, and Applications. *J. Drug Deliv. Sci. Technol.* **2019**, *53*, 101174. [[CrossRef](#)]
2. Rana, A.; Yadav, K.; Jagadevan, S. A Comprehensive Review on Green Synthesis of Nature-Inspired Metal Nanoparticles: Mechanism, Application and Toxicity. *J. Clean. Prod.* **2020**, *272*, 122880. [[CrossRef](#)]
3. Bao, Z.; Lan, C.Q. Advances in Biosynthesis of Noble Metal Nanoparticles Mediated by Photosynthetic Organisms—A Review. *Colloids Surfaces B Biointerfaces* **2019**, *184*, 110519. [[CrossRef](#)]
4. Alavi, M.; Kamarasu, P.; McClements, D.J.; Moore, M.D. Metal and Metal Oxide-Based Antiviral Nanoparticles: Properties, Mechanisms of Action, and Applications. *Adv. Colloid Interface Sci.* **2022**, *306*, 102726. [[CrossRef](#)] [[PubMed](#)]

5. Mishra, A.; Pradhan, D.; Halder, J.; Biswasroy, P.; Rai, V.K.; Dubey, D.; Kar, B.; Ghosh, G.; Rath, G. Metal Nanoparticles against Multi-Drug-Resistance Bacteria. *J. Inorg. Biochem.* **2022**, *237*, 111938. [[CrossRef](#)]
6. Beyene, H.D.; Werkneh, A.A.; Bezabh, H.K.; Ambaye, T.G. Synthesis Paradigm and Applications of Silver Nanoparticles (AgNPs), a Review. *Sustain. Mater. Technol.* **2017**, *13*, 18–23. [[CrossRef](#)]
7. Jorge de Souza, T.A.; Rosa Souza, L.R.; Franchi, L.P. Silver Nanoparticles: An Integrated View of Green Synthesis Methods, Transformation in the Environment, and Toxicity. *Ecotoxicol. Environ. Saf.* **2019**, *171*, 691–700. [[CrossRef](#)]
8. Khodashenas, B.; Ghorbani, H.R. Synthesis of Silver Nanoparticles with Different Shapes. *Arab. J. Chem.* **2019**, *12*, 1823–1838. [[CrossRef](#)]
9. Fu, L.M.; Hsu, J.H.; Shih, M.K.; Hsieh, C.W.; Ju, W.J.; Chen, Y.W.; Lee, B.H.; Hou, C.Y. Process Optimization of Silver Nanoparticle Synthesis and Its Application in Mercury Detection. *Micromachines* **2021**, *12*, 1123. [[CrossRef](#)]
10. Pinto, R.J.B.; Nasirpour, M.; Carrola, J.; Oliveira, H.; Freire, C.S.R.; Duarte, I.F. *And Therapeutic Applications and Nanocomposites*; Elsevier Inc.: Amsterdam, The Netherlands, 2017; ISBN 9780323527330.
11. Yun, J.E.; Lee, D.G. *Silver Nanoparticles: A Novel Antimicrobial Agent*; Elsevier Inc.: Amsterdam, The Netherlands, 2017; ISBN 9780323527347.
12. Durán, N.; Durán, M.; de Jesus, M.B.; Seabra, A.B.; Fávaro, W.J.; Nakazato, G. Silver Nanoparticles: A New View on Mechanistic Aspects on Antimicrobial Activity. *Nanomedicine Nanotechnology, Biol. Med.* **2016**, *12*, 789–799. [[CrossRef](#)]
13. Mosselhy, D.A.; El-Aziz, M.A.; Hanna, M.; Ahmed, M.A.; Husien, M.M.; Feng, Q. Comparative Synthesis and Antimicrobial Action of Silver Nanoparticles and Silver Nitrate. *J. Nanoparticle Res.* **2015**, *17*, 1–10. [[CrossRef](#)]
14. Ali, J.; Ali, N.; Wang, L.; Waseem, H.; Pan, G. Revisiting the Mechanistic Pathways for Bacterial Mediated Synthesis of Noble Metal Nanoparticles. *J. Microbiol. Methods* **2019**, *159*, 18–25. [[CrossRef](#)] [[PubMed](#)]
15. Abou El-Nour, K.M.M.; Eftaiha, A.; Al-Warthan, A.; Ammar, R.A.A. Synthesis and Applications of Silver Nanoparticles. *Arab. J. Chem.* **2010**, *3*, 135–140. [[CrossRef](#)]
16. Deshmukh, S.P.; Patil, S.M.; Mullani, S.B.; Delekar, S.D. Silver Nanoparticles as an Effective Disinfectant: A Review. *Mater. Sci. Eng. C* **2019**, *97*, 954–965. [[CrossRef](#)] [[PubMed](#)]
17. Alharbi, N.S.; Alsubhi, N.S.; Felimban, A.I. Green Synthesis of Silver Nanoparticles Using Medicinal Plants: Characterization and Application. *J. Radiat. Res. Appl. Sci.* **2022**, *15*, 109–124. [[CrossRef](#)]
18. Yu, Y.; Zhou, Z.; Huang, G.; Cheng, H.; Han, L.; Zhao, S.; Chen, Y.; Meng, F. Purifying Water with Silver Nanoparticles (AgNPs)-Incorporated Membranes: Recent Advancements and Critical Challenges. *Water Res.* **2022**, *222*, 118901. [[CrossRef](#)]
19. Liu, J.F.; Yu, S.J.; Yin, Y.G.; Chao, J.B. Methods for Separation, Identification, Characterization and Quantification of Silver Nanoparticles. *TrAC Trends Anal. Chem.* **2012**, *33*, 95–106. [[CrossRef](#)]
20. Bhardwaj, A.K.; Sundaram, S.; Yadav, K.K.; Srivastav, A.L. An Overview of Silver Nano-Particles as Promising Materials for Water Disinfection. *Environ. Technol. Innov.* **2021**, *23*, 101721. [[CrossRef](#)]
21. Khan, S.A.; Jain, M.; Pandey, A.; Pant, K.K.; Ziora, Z.M.; Blaskovich, M.A.T.; Shetti, N.P.; Aminabhavi, T.M. Leveraging the Potential of Silver Nanoparticles-Based Materials towards Sustainable Water Treatment. *J. Environ. Manage.* **2022**, *319*, 115675. [[CrossRef](#)]
22. Esmaeili Bidhendi, M.; Parandi, E.; Mahmoudi Meymand, M.; Sereshti, H.; Rashidi Nodeh, H.; Joo, S.W.; Vasseghian, Y.; Mahmoudi Khatir, N.; Rezaia, S. Removal of Lead Ions from Wastewater Using Magnesium Sulfide Nanoparticles Caged Alginate Microbeads. *Environ. Res.* **2023**, *216*, 114416. [[CrossRef](#)]
23. Alipour Atmianlu, P.; Badpa, R.; Aghabalaie, V.; Baghdadi, M. A Review on the Various Beds Used for Immobilization of Nanoparticles: Overcoming the Barrier to Nanoparticle Applications in Water and Wastewater Treatment. *J. Environ. Chem. Eng.* **2021**, *9*, 106514. [[CrossRef](#)]
24. Eltz, F.Z.; Vebber, M.C.; Aguzzoli, C.; Machado, G.; Da Silva Crespo, J.; Giovanela, M. Preparation, Characterization and Application of Polymeric Thin Films Containing Silver and Copper Nanoparticles with Bactericidal Activity. *J. Environ. Chem. Eng.* **2020**, *8*, 1–14. [[CrossRef](#)]
25. Wang, R.; Zhao, P.; Yu, R.; Jiang, J.; Liang, R.; Liu, G. Cost-Efficient Collagen Fibrous Aerogel Cross-Linked by Fe (III) /Silver Nanoparticle Complexes for Simultaneously Degrading Antibiotics, Eliminating Antibiotic-Resistant Bacteria, and Adsorbing Heavy Metal Ions from Wastewater. *Sep. Purif. Technol.* **2022**, *303*. [[CrossRef](#)]
26. Najafpoor, A.; Norouzian-Ostad, R.; Alidadi, H.; Rohani-Bastami, T.; Davoudi, M.; Barjasteh-Askari, F.; Zanganeh, J. Effect of Magnetic Nanoparticles and Silver-Loaded Magnetic Nanoparticles on Advanced Wastewater Treatment and Disinfection. *J. Mol. Liq.* **2020**, *303*, 112640. [[CrossRef](#)]
27. Wu, Z.; Tang, S.; Deng, W.; Luo, J.; Wang, X. Antibacterial Chitosan Composite Films with Food-Inspired Carbon Spheres Immobilized AgNPs. *Food Chem.* **2021**, *363*, 130342. [[CrossRef](#)] [[PubMed](#)]
28. Sadhu, S.D.; Garg, M.; Kumar, A. *Major Environmental Issues and New Materials*; Elsevier Inc.: Amsterdam, The Netherlands, 2018. [[CrossRef](#)]
29. Tamayo, L.; Palza, H.; Bejarano, J.; Zapata, P.A. *Polymer Composites with Metal Nanoparticles: Synthesis, Properties, and Applications. Synthesis, Properties, and Applications*; Elsevier Inc.: Amsterdam, The Netherlands, 2018; ISBN 9780128140659.
30. Soetaredjo, F.E.; Ismajli, S.; Foe, K.; Yi-Hsu, J. *Recent Advances in the Application of Polymer-Based Nanocomposites for Removal of Hazardous Substances from Water and Wastewater*; Elsevier Inc.: Amsterdam, The Netherlands, 2018. [[CrossRef](#)]

31. Potara, M.; Focsan, M.; Craciun, A.M.; Botiz, I.; Astilean, S. *Polymer-Coated Plasmonic Nanoparticles for Environmental Remediation: Synthesis, Functionalization, and Properties*; Elsevier Inc.: Amsterdam, The Netherlands, 2018. [\[CrossRef\]](#)
32. Raota, C.S.; Cerbaro, A.F.; Salvador, M.; Delamare, A.P.L.; Echeverrigaray, S.; Da Silva Crespo, J.; Da Silva, T.B.; Giovanela, M. Green Synthesis of Silver Nanoparticles Using an Extract of Ives Cultivar (*Vitis Labrusca*) Pomace: Characterization and Application in Wastewater Disinfection. *J. Environ. Chem. Eng.* **2019**, *7*, 103383. [\[CrossRef\]](#)
33. Qin, Y.; Liu, Y.; Yuan, L.; Yong, H.; Liu, J. Preparation and Characterization of Antioxidant, Antimicrobial and PH-Sensitive Films Based on Chitosan, Silver Nanoparticles and Purple Corn Extract. *Food Hydrocoll.* **2019**, *96*, 102–111. [\[CrossRef\]](#)
34. Rhim, J.W.; Hong, S.I.; Park, H.M.; Ng, P.K.W. Preparation and Characterization of Chitosan-Based Nanocomposite Films with Antimicrobial Activity. *J. Agric. Food Chem.* **2006**, *54*, 5814–5822. [\[CrossRef\]](#)
35. Shah, A.; Hussain, I.; Murtaza, G. Chemical Synthesis and Characterization of Chitosan/Silver Nanocomposites Films and Their Potential Antibacterial Activity. *Int. J. Biol. Macromol.* **2018**, *116*, 520–529. [\[CrossRef\]](#)
36. Liang, J.; Wang, J.; Li, S.; Xu, L.; Wang, R.; Chen, R.; Sun, Y. The Size-Controllable Preparation of Chitosan/Silver Nanoparticle Composite Microsphere and Its Antimicrobial Performance. *Carbohydr. Polym.* **2019**, *220*, 22–29. [\[CrossRef\]](#)
37. Dai, X.; Li, S.; Li, S.; Ke, K.; Pang, J.; Wu, C.; Yan, Z. High Antibacterial Activity of Chitosan Films with Covalent Organic Frameworks Immobilized Silver Nanoparticles. *Int. J. Biol. Macromol.* **2022**, *202*, 407–417. [\[CrossRef\]](#) [\[PubMed\]](#)
38. Mohamed, N.; Madian, N.G. Evaluation of the Mechanical, Physical and Antimicrobial Properties of Chitosan Thin Films Doped with Greenly Synthesized Silver Nanoparticles. *Mater. Today Commun.* **2020**, *25*, 101372. [\[CrossRef\]](#)
39. Zhou, L.; Zhao, X.; Li, M.; Yan, L.; Lu, Y.; Jiang, C.; Liu, Y.; Pan, Z.; Shi, J. Antibacterial and Wound Healing–Promoting Effect of Sponge-like Chitosan-Loaded Silver Nanoparticles Biosynthesized by Iturin. *Int. J. Biol. Macromol.* **2021**, *181*, 1183–1195. [\[CrossRef\]](#)
40. Shankar, S.; Khodaei, D.; Lacroix, M. Effect of Chitosan/Essential Oils/Silver Nanoparticles Composite Films Packaging and Gamma Irradiation on Shelf Life of Strawberries. *Food Hydrocoll.* **2021**, *117*, 106750. [\[CrossRef\]](#)
41. Sartori, P.; Possan, A.L.; Jonko, E.; Giovanela, M. Silver Nitrate from Recovered Silver of Spent Ag<sub>2</sub>O Button Cells: Synthesis and Characterization. *J. Sustain. Metall.* **2020**, *6*, 557–562. [\[CrossRef\]](#)
42. Jana, N.R.; Gearheart, L.; Murphy, C.J. Wet Chemical Synthesis of Silver Nanorods and Nanowires of Controllable Aspect Ratio. *Chem. Commun.* **2001**, *2001*, 617–618. [\[CrossRef\]](#)
43. Henglein, A.; Giersig, M. Jp9925334.Pdf. *J. Phys. Chem. B* **1999**, *46556*, 9533–9539. [\[CrossRef\]](#)
44. AOAC. *AOAC Official Method 991.14, Coliform and Escherichia Coli Counts in Foods—Dry Rehydratable Film*, 20th ed.; AOAC: Rockville, MD, USA, 2016.
45. Rice, E.W.; Baird, R.B.; Eaton, A.D. (Eds.) *Standard Methods for the Examination of Water and Wastewater*, 23rd ed.; American Public Health Association, American Water Works Association, Water Environment Federation: Washington, DC, USA, 2017; ISBN 9780875532875.
46. Takeno, N. Atlas of Eh-PH Diagrams Intercomparison of Thermodynamic Databases. In *National Institute of Advanced Industrial Science and Technology Tokyo*; AIST: Tokyo, Japan, 2005; p. 285. ISBN 978-0915567980.
47. Norouzi, A.; Adeli, M.; Zakeri, A. An Innovative Hydrometallurgical Process for the Production of Silver Nanoparticles from Spent Silver Oxide Button Cells. *Sep. Purif. Technol.* **2020**, *248*, 117015. [\[CrossRef\]](#)
48. Biao, L.; Tan, S.; Wang, Y.; Guo, X.; Fu, Y.; Xu, F.; Zu, Y.; Liu, Z. Synthesis, Characterization and Antibacterial Study on the Chitosan-Functionalized Ag Nanoparticles. *Mater. Sci. Eng. C* **2017**, *76*, 73–80. [\[CrossRef\]](#)
49. Zhao, X.; Tian, R.; Zhou, J.; Liu, Y. Multifunctional Chitosan/Grape Seed Extract/Silver Nanoparticle Composite for Food Packaging Application. *Int. J. Biol. Macromol.* **2022**, *207*, 152–160. [\[CrossRef\]](#)
50. Sarkar, R.; Anil, K.C.; Kumbhakar, P.; Mandal, T. Aqueous Synthesis and Antibacterial Activity of Silver Nanoparticles against *Pseudomonas Putida*. *Mater. Today Proc.* **2019**, *11*, 686–694. [\[CrossRef\]](#)
51. Chahar, V.; Sharma, B.; Shukla, G.; Srivastava, A.; Bhatnagar, A. Study of Antimicrobial Activity of Silver Nanoparticles Synthesized Using Green and Chemical Approach. *Colloids Surfaces A Physicochem. Eng. Asp.* **2018**, *554*, 149–155. [\[CrossRef\]](#)
52. Bertin, M.; Perottoni, C.A. Efeito Da Ressonância Plasmônica Sobre o Espectro de Absorção de Nanopartículas Metálicas. *Sci. CUM Ind.* **2020**, *8*, 12–24. [\[CrossRef\]](#)
53. Htwe, Y.Z.N.; Chow, W.S.; Suda, Y.; Mariatti, M. Effect of Silver Nitrate Concentration on the Production of Silver Nanoparticles by Green Method. *Mater. Today Proc.* **2019**, *17*, 568–573. [\[CrossRef\]](#)
54. Dong, X.; Ji, X.; Wu, H.; Zhao, L.; Li, J.; Yang, W. Shape Control of Silver Nanoparticles by Stepwise Citrate Reduction. *J. Phys. Chem. C* **2009**, *113*, 6573–6576. [\[CrossRef\]](#)
55. Gervais, C.; Grissom, C.A.; Little, N.; Wachowiak, M.J. Cleaning Marble with Ammonium Citrate. *Stud. Conserv.* **2010**, *55*, 164–176. [\[CrossRef\]](#)
56. Shen, Z.; Liu, J.; Hu, F.; Liu, S.; Cao, N.; Sui, Y.; Zeng, Q.; Shen, Y. Bottom-up Synthesis of Cerium-Citric Acid Coordination Polymers Hollow Microspheres with Tunable Shell Thickness and Their Corresponding Porous CeO<sub>2</sub> Hollow Spheres for Pt-Based Electrocatalysts. *CrystEngComm* **2014**, *16*, 3387–3394. [\[CrossRef\]](#)
57. Salazar-Bryam, A.M.; Yoshimura, I.; Santos, L.P.; Moura, C.C.; Santos, C.C.; Silva, V.L.; Lovaglio, R.B.; Costa Marques, R.F.; Jafelicci Junior, M.; Contiero, J. Silver Nanoparticles Stabilized by Ramnolipids: Effect of PH. *Colloids Surfaces B Biointerfaces* **2021**, *205*, 111883. [\[CrossRef\]](#)

58. Mohaghegh, S.; Osouli-Bostanabad, K.; Nazemiyeh, H.; Javadzadeh, Y.; Parvizpur, A.; Barzegar-Jalali, M.; Adibkia, K. A Comparative Study of Eco-Friendly Silver Nanoparticles Synthesis Using Prunus Domestica Plum Extract and Sodium Citrate as Reducing Agents. *Adv. Powder Technol.* **2020**, *31*, 1169–1180. [[CrossRef](#)]
59. Fayaz, A.M.; Balaji, K.; Girilal, M.; Yadav, R.; Kalaichelvan, P.T.; Venketesan, R. Biogenic Synthesis of Silver Nanoparticles and Their Synergistic Effect with Antibiotics: A Study against Gram-Positive and Gram-Negative Bacteria. *Nanomedicine Nanotechnology, Biol. Med.* **2010**, *6*, 103–109. [[CrossRef](#)]
60. Jung, J.; Kasi, G.; Seo, J. Development of Functional Antimicrobial Papers Using Chitosan/Starch-Silver Nanoparticles. *Int. J. Biol. Macromol.* **2018**, *112*, 530–536. [[CrossRef](#)] [[PubMed](#)]
61. Hajji, S.; Khedir, S.B.; Hamza-Mnif, I.; Hamdi, M.; Jedidi, I.; Kallel, R.; Boufi, S.; Nasri, M. Biomedical Potential of Chitosan-Silver Nanoparticles with Special Reference to Antioxidant, Antibacterial, Hemolytic and in Vivo Cutaneous Wound Healing Effects. *Biochim. Biophys. Acta Gen. Subj.* **2019**, *1863*, 241–254. [[CrossRef](#)] [[PubMed](#)]
62. Morsi, R.E.; Alsabagh, A.M.; Nasr, S.A.; Zaki, M.M. Multifunctional Nanocomposites of Chitosan, Silver Nanoparticles, Copper Nanoparticles and Carbon Nanotubes for Water Treatment: Antimicrobial Characteristics. *Int. J. Biol. Macromol.* **2017**, *97*, 264–269. [[CrossRef](#)] [[PubMed](#)]
63. Khan, F.; Pham, D.T.N.; Oloketuyi, S.F.; Manivasagan, P.; Oh, J.; Kim, Y.M. Chitosan and Their Derivatives: Antibiofilm Drugs against Pathogenic Bacteria. *Colloids Surfaces B Biointerfaces* **2020**, *185*, 110627. [[CrossRef](#)]
64. Bondarenko, O.M.; Sihtmäe, M.; Kuzmičiova, J.; Ragelienė, L.; Kahru, A.; Daugelavičius, R. Bacterial Plasma Membrane Is the Main Cellular Target of Silver Nanoparticles in *Escherichia coli* and *Pseudomonas Aeruginosa*. *bioRxiv* **2018**, *13*, 6779–6790.
65. Zarpelon, F.; Galiotto, D.; Aguzolli, C.; Carli, L.N.; Figueroa, C.A.; Baumvol, I.J.R.; Machado, G.; Crespo, J.D.S.; Giovanela, M. Removal of Coliform Bacteria from Industrial Wastewaters Using Polyelectrolytes/Silver Nanoparticles Self-Assembled Thin Films. *J. Environ. Chem. Eng.* **2016**, *4*, 137–146. [[CrossRef](#)]
66. Lovatel, R.H.; Neves, R.M.; Oliveira, G.R.; Mauler, R.S.; Crespo, J.S.; Carli, L.N.; Giovanela, M. Disinfection of Biologically Treated Industrial Wastewater Using Montmorillonite/Alginate/Nanosilver Hybrids. *J. Water Process Eng.* **2015**, *7*, 273–279. [[CrossRef](#)]
67. World Health Organization. *Guidelines for Drinking-Water Quality*, 4th ed.; World Health Organization: Geneva, Switzerland, 2022; ISBN 978-92-4-004506-4.

**Disclaimer/Publisher's Note:** The statements, opinions and data contained in all publications are solely those of the individual author(s) and contributor(s) and not of MDPI and/or the editor(s). MDPI and/or the editor(s) disclaim responsibility for any injury to people or property resulting from any ideas, methods, instructions or products referred to in the content.